ORIGINAL ARTICLE

Chest Wall Motion Tracking By Contactless Optical Single Camera-Based Method Using Virtual Markers, a Feasibility Study

Mohammad Ali Bijari, Ahmad Eesmaili Torshabi *

Faculty of Sciences and Modern Technologies, Graduate University of Advanced Technology, Kerman, Iran

*Corresponding Author: Ahmad Eesmaili Torshabi
Email: ahmad4958@gmail.com

Received: 11 December 2023 / Accepted: 19 May 2024

Abstract

Purpose: Real-time motion tracking of the thorax region of patient's body is a main issue in various parts of medical fields, such as radiotherapy. Several strategies were proposed by using different monitoring hardware. In this work, a contactless method is proposed using an optical camera to trace breathing motion by implementing virtual markers defined on the chest area. A detailed algorithm has been developed to analyze the video frames and track each virtual point in real real-time fashion.

Materials and Methods: In this work, Python program and its OpenCV library have been utilized for breathing motion, two-dimensionally. Database utilized in this work is motion data taken from the breathing motion of a real volunteer. The motion data was captured using a cellphone optical camera, and the gathered data was transferred to the in-room computer system by means of WiFi. It's worth mentioning that 15 virtual test points were determined using Artificial Intelligence concept of Python inside the chest area.

Results: Final results show that the performance accuracy of the monitoring proposed idea is acceptable. The chest area is determined automatically and will be variable for each patient, uniquely. Various normal and deep breathings were tested in real time at different respiration frequencies. For example, two-dimensional motion displacements of a test point are 4.75 and 7.15 mm for normal and deep breathing, respectively.

Conclusion: The main robustness of the proposed motion tracking method is simplicity, contactless, and using virtual markers determination, while real infra-red markers are currently used clinically by being located on patient's chest skin.

Keywords: Motion Capture; Optical Devices; Virtual Markers; Targeted Radiotherapy.

DOI: https://doi.org/10.18502/fbt.v13i1.20770

1. Introduction

In recent decades, radiotherapy has been well known as a curative and palliative strategy for killing the tumor cells and eliminating cancer [1-4]. In radiotherapy of dynamic tumors, while motion is a challenging issue, there will be potentially significant difference between the planned dose measured during the Treatment Planning System and the actual dose delivered into the tumor volume [5].

Dynamic tumors are located in the thorax region of the patient's body and move due to breathing phenomena, heartbeat, gastrointestinal system, and filling/emptying the bladder and rectum, known as intra-fractional motions [6-8]. Apart from PTV (Planning Target Volume) defined for static tumors, ITV (Internal Target Volume) has already been specified for moving tumors to cover the tumor motion amplitude, three-dimensionally [9-14]. Therefore, in prior conventional radiotherapy of moving tumors, PTV includes ITV, consisting of the total tumor motion region, resulting remarkable dose to healthy tissues around the tumor volume. This will be the main concern while OARs (Organ at Risk) are located near the tumor site and may give rise to secondary cancers [15-18].

Several strategies have been proposed to manage motion issue at radiotherapy ranging from breath holding [19-21], real-time tumor tracking using external surrogates [22-35], and X-ray fluoroscopy [36, 37]. At thebreath-holding method, patient cooperation is needed, while most patients, such as old or children, are not able to proceed with the treatment process. Moreover, this strategy has a non-negligible error while holding the breaths are not essentially similar to each other. At the latter strategy, using a fluoroscopy system, the amount of additional imaging dose received by the patient is significant which is against the ALARA (As Low As Reasonably Achievable) principle [38-40]. Although the fluoroscopy system in the treatment room gives real coordinates of tumor volume continuously, if the contrast is not an issue [37]. It should be noted that in both latter methods, an internal clip is implanted inside or near the tumor volume in order to enhance the contrast [41-44].

At external surrogates radiotherapy, a prediction model is utilized to estimate tumor position three-dimensionally as function of external rib cage motion in real time [23, 45-48]. To do this, hardware systems are installed in the treatment room to monitor the rib cage and abdomen motion as external data and tumor motion as internal data, synchronously. The prediction model is first trained by finding a proper correlation between the external and internal motions data, extracted at the pre-treatment step. It should be noted that three to five markers are located on the thorax region of the patient's body, representing external motions. The information of internal tumor position is determined by means of a stereoscopic X-ray imaging system [49, 50]. It's worth mentioning that the performance accuracy of the model is intermittently checked by taking X-ray images during the treatment session. Several predictive models have been proposed in different literature ranging from linear to combined neuro fuzzy correlation models [34].

In radiotherapy based on surrogates, external data extraction from the thorax region is one of the main components using noninvasive strategies. Several works have been done to gather external motion data, such as respiration belt [51], respiration capacitor [52], ultrasonic sensors [53], Doppler radar [54], and Optical cameras, such as infrared and so on [55-58].

Carlo *et al.* [59] proposed using non-contact optical sensors such as commercial cameras due to some advantages as low cost and easy to use. L.Tarassenko *et al.* [60] have introduced the same strategy, and they used variation in intensity of RGB image pixels through a selected region of interest. Michael *et al.* [56] used optical cameras for motion monitoring using Optical Flow algorithms for respiratory motion tracking. In a later study, Lucas Kanade's local optical flow has been used over the entire image. The drawback of this work is the long computational time.

In this study, a simple and feasible method was proposed based on a common available optical camera to track chest wall motion in real time. In the proposed idea, the infra-red markers, which are currently used clinically [61], are removed and a contactless strategy based on virtual points is utilized as an alternative representing external markers.

Along with different methods and sensors for motion capture, those which are contactless and [62]

have remarkable priority. Using a contactless monitoring sensor, there is no need for patient cooperation, and the patient is also safe against some skin issues caused by markers [42, 63].

After data gathering from the camera, the extracted motion data are automatically saved as log files, cumulatively. It should be noted that a proper algorithm based on Optical Flow (OF) [43-46] was developed at the Python software package to enable operators to determine the desired area of the thorax region, the number of virtual points, and the coordinates of each point. in order to further simplify, the chest wall location can be automatically detected using Artificial Intelligence (AI) methods.

Final obtained results show that the Region Of Interest (ROI) of captured images for motion tracking is based on the basis an artificial intelligence pre-defined in Python, automatically. Due to this, OF will not be implemented on the entire image data and therefore the computational time of the final program will be significantly reduced which yields motion monitoring in real-time mode. Furthermore, by comparison to the other methods, the proposed idea is superior because of its simplicity and feasibility by means of e.g., mobile cellphone cameras.

2. Materials and Methods

In the radiation treatment of moving tumors, external surrogates radiotherapy is now implemented clinically. In this method correlation model is responsible for tracking tumor motion using external markers' motion. Figure 1 shows the configuration (step 1), performance (step 2), and testing (step 3) of the model. As mentioned, internal tumor motion data is correlated with external motion data extracted from optical cameras at the pre-treatment step for model training. Then the configured model is ready to use external data as input.

As seen in this figure, external motion data extraction is one of the most important parts that should be performed with appropriate accuracy, which is the main focus of this study.

2.1. Python, OpenCV & Optical Flow

Python is a user-friendly Object-oriented and high-level programming language that is very attractive for use in various fields ranging from computer-aided requirements, mobile applications development, and web page design (Python Ver.3.10.7). Moreover, Python includes a very strong in-accessible modules library that enables us to import and export them at each desired project, easily.

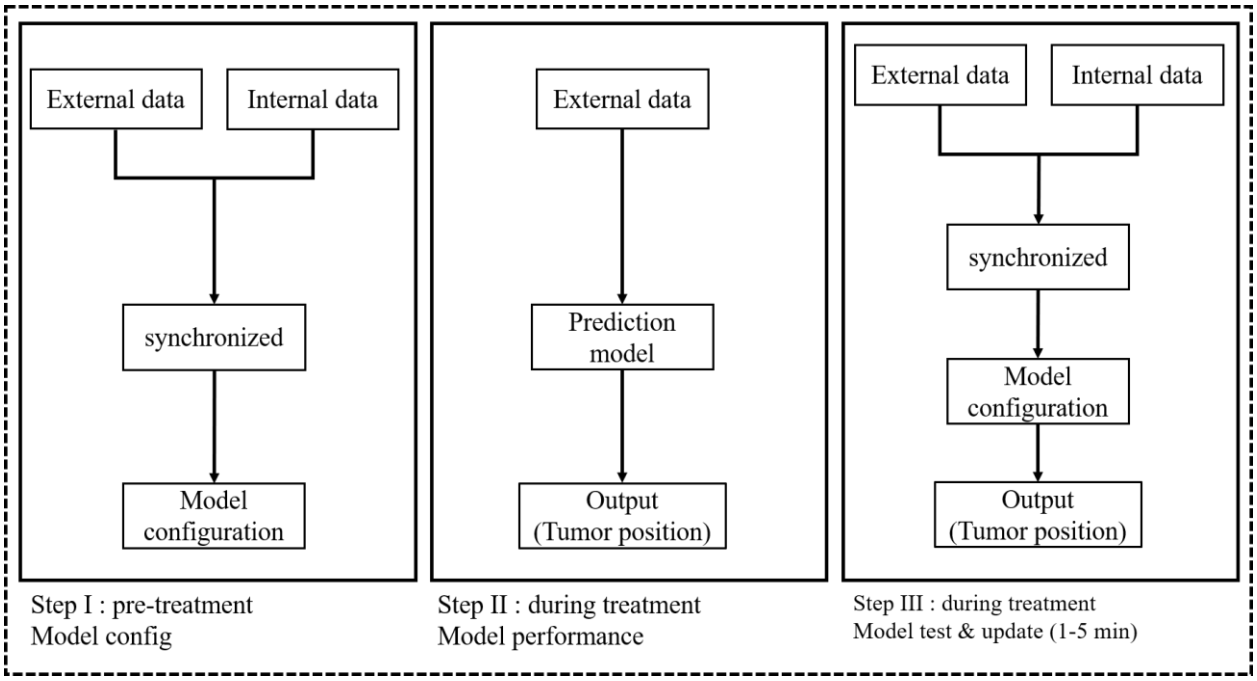

Figure 1. Correlation model diagram for tumor motion tracking at external surrogates radiotherapy

OpenCV (Open Computer Vision, Ver 4.6.0) is an open-source library that uses more than 500 algorithms to analyze photos and videos for different aims. Firstly, introduced in 1999 by Intel to improve the development of image processing applications. In this study, OpenCv library was added to Python and OF was then implemented on the given images to detect the external thorax motion of each patient's body.

Optical flow algorithm is a commonly available dedicated code to follow an object's motion via given frequent images of that object. The output of OF depicts a two-dimensional vector showing the movement of an object from one point to another. The OF algorithm is working on the basis of two following assumptions: Firstly, intensities of the object pixels don't change in consecutive frames, and secondly, nearby pixels have similar movement.

Considering I(x, y, t) represents the Intensity variable, in the first frame after a short period of time (Equation 1):

$$I(x,y,t) = I(x+dx, y+dy, t+dt) \quad (1)$$

Where dx and dy are displacements on the X and Y axes, and dt is the elapsed time. The simplification of the above equation is as follows (Equation 2):

$$f_x u + f_y \vartheta + f_t \quad (2)$$

Where (Equation 3),

$$f_x = \frac{\partial f}{\partial x}; f_y \frac{\partial f}{\partial y}$$

$$u = \frac{dx}{dt}; \vartheta \frac{dy}{dt} \quad (3)$$

Which fx and fy are picture gradients, and similarly and ft will be the time gradient. since the optical flow is an equation with two unknown parameters (u, ϑ), it is unsolvable [64]. So, there are different methods to solve the equation that one of which is through the Lucas-Kanade method.

The Lucas-Kanade assumes that if all nearby pixels in a 3*3 matrix with the same movement, equation 2-2 is repeated for all 9 points in that matrix. The new optical flow equation is (Equation 4):

$$\begin{matrix} u \\ \vartheta \end{matrix} = \begin{bmatrix} \sum_i {f_{xi}}^2 & \sum_i f_{xi} f_{yi} \\ \sum_i f_{xi} f_{yi} & \sum_i {f_{yi}}^2 \end{bmatrix}^{-1} \begin{matrix} -\sum_i f_{xi} f_{ti} \\ -\sum_i f_{yi} f_{ti} \end{matrix} \quad (4)$$

So, there will be 9 equations with 2 unknown parameters that will be solvable [65-67].

The whole diagram of our developed program is shown in Figure 2.

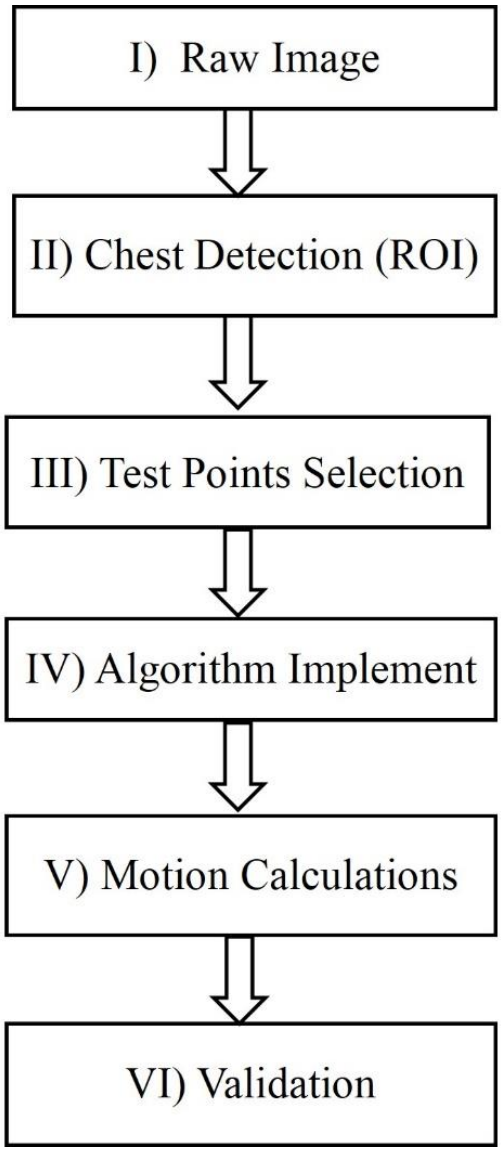

Figure 2. Block diagram of the developed program

2.2. Chest Region Detection as ROI & Test Points

In the first section, the video input file has been initialized which results in an infinite loop for capturing the frames of inconming video (raw Images Figure 2, block No. 1). It should be noted that, there is

an open-access Media Pipe Library at AI part of Paython represrnting human body pose detection by means of 32 landmark (Figure 3).

By applying this ability of Paython AI on our incoming video frames, two landmarks located on right shoulder (Figure 3, landmark No. 11) and left shoulder (Figure 3, landmark No. 12) of the patient's body are detected automatically. Then, the chest surface region will be automatically determined using a specific area located at the lower part of two 11 and 12 landmarks as a benchmark. It should be noted that the chest region detection is done on the first video frame assuming no unwanted motion of the patient body (Figure 2, Block No. 2). Our developed program has been done on our case, and Figure 4 shows the ROI as rectangular red.

After chest detection, the next step includes test points coordinates at ROI (Figure 2, Block No. 3). Test points represent some specific virtual coordinates distributed at ROI with similar distances to each other. Figure 5 depicts 15 test points in the chest area of our case. It should be noted that the above test points are utilized as input for our developed optical flow algorithm to trace test points displacements as a function of time. Also due to using testpoints as an input of the motion tracking algorithm the overall computional time will be decreased. Since each patient has its unique body pose, it's worth mentioning that our developed program is able to be personalized for each patient on a case-by-case basis, mainly at two sections: I) shoulder landmarks detection and II) test points distribution.

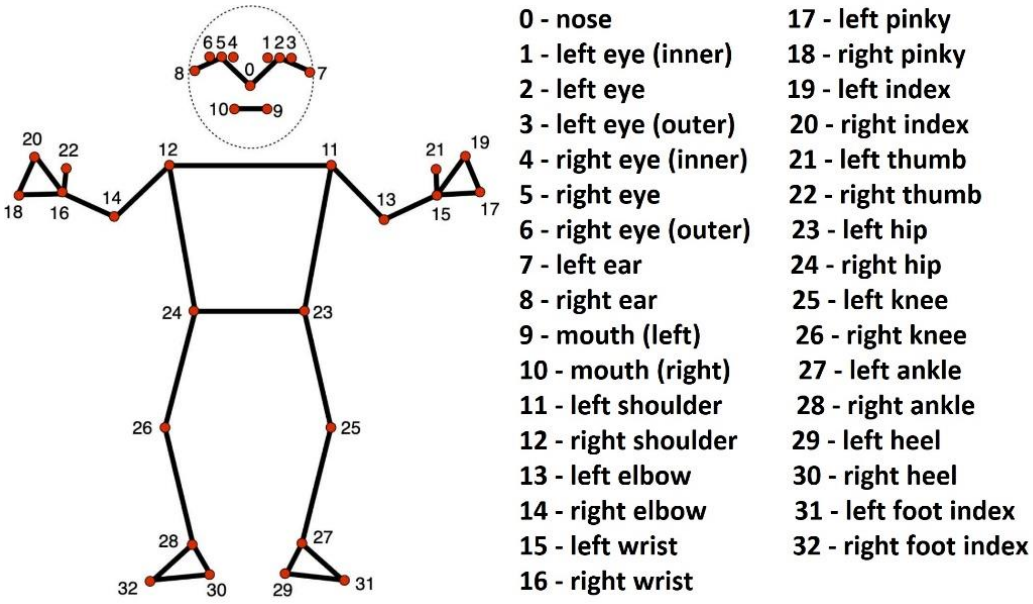

Figure 3. 32 media pipe landmarks pre-defined at Phayton AI human body pose detection

Figure 4. chest area detection as ROI using Python AI subroutine

2.3. Data Gathering and Optical Flow Performance

In this work, the motion data of the chest region was captured by means of an optical camera of the Sumsung Galaxy A33 cellphone. The characteristics of the main camera used in this study are 48 megapixels. Then, the captured video was transferred into the computer system with a local WiFi interface application as real-timein order to avoid time latency of the system.

After selection of the test points at block No. 3, the OF algorithm is ready to execute on the motion database extracted by test points displacement. To do this, the BGR frames taken by the optical camera should be converted to a Gray scale as acceptable images as required for the Lucas-Kanade function in OF. The optical flow algorithm works on the basis motion displacement of test points between two old and current frames. Due to this, the first frame that is used for ROI detection can also be utilized as an old frame for OF performance.

During OF implementation, the latest taken frame is considerd as new image and therefore 15 test points displacments calculation is done by repeating OF execution, using prior old frame. After gathering the coordinates of old and new points from the OF algorithm, it is needed to calculate the motion displacement. According to Figure 5, assuming one of 15 points (as pt1), motion displacement is calculated using the new point (as pt2) through the Pythagorean theorem (Figure 6).

It should be noted that since the location of test points is in a pixel mode, the result of movement calculation will be in pixels. so that, as the final step, the conversion from pixels to millimeters is required.BecauseBecause after extracting motion data, it is imported as external data into the correlation model, and since the output of that model is in the millimeter system, the input of it should be in the millimeter system which is the output of this program.

2.4. Test and Validation of the Developed Program

As mentioned, the calculated movement should be converted from pixel to millimeter. To do this, a pixel/millimeter ratio as a metric tool is needed for this conversion. There is a specific library in the openCV module of Python that can detect some commonly available markers known as Aruco markers (Figure 7).

In this work, we chose an Aruco marker with a total 50×50 millimeter dimension for installing on a patient vest. This Marker enables us to convert the number of pixels into the millimeters. If the length and width of the marker in pixel sizes called PL and PW, and similarly their length and width in millimeters called ML and MW, the total displacement in millimeter size(MT) is calculated as below, where final displacement in pixel size called PT as shown in Equation 5:

$$M_S = M_L \times M_W \ , \qquad P_S = P_L \times P_W$$
$$pm\ ratio = \frac{M_S}{P_S} \tag{5}$$
$$M_T = P_T \times pm\ ratio$$

Figure 5. 15 test points distributed inside the ROI

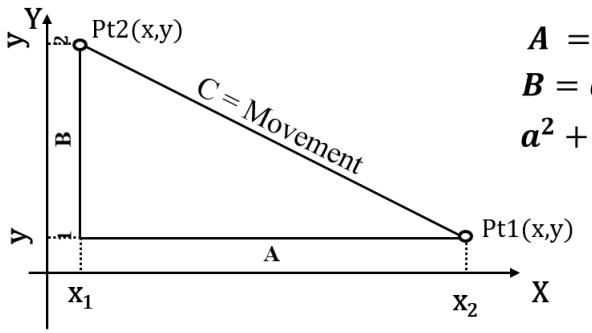

$$\left.\begin{aligned} A &= dx = x_2 - x_1 \\ B &= dy = y_2 - y_1 \\ a^2 + b^2 &= c^2 \end{aligned}\right\} \Longrightarrow C = \sqrt{a^2 + b^2}$$

Figure 6. calculating total movement (distance) through the Pythagorean theorem

(d_x and d_y represent horizontal and vertical displacement, respectively)

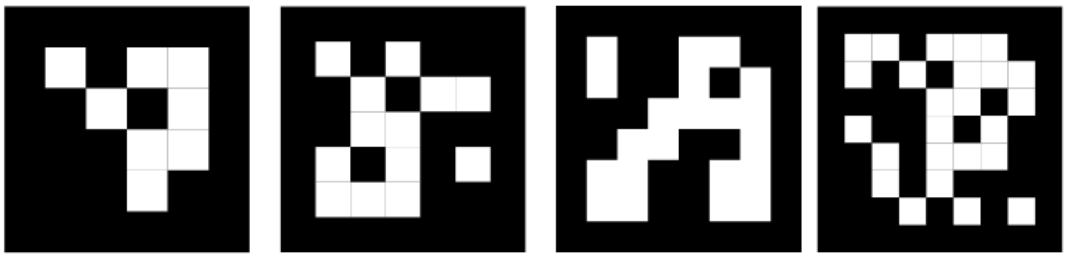

Figure 7. Four typical Aruco markers

that is the way used for validating and converting displacement data from pixels to millimeters. Since there is a specific package in Python for the detection of some special markers called “aruco marker”, those kinds of marker have been used for data conversion. Considering that the millimeter to pixel ratio is different at any distance from the camera, this Technique was used for more accurate results.

Figure 8 shows the validity process of the proposed idea using an Aruco marker installed on the vest of our case as a volunteer. The developed program will convert pixel size to millimeters using the radius mentioned above. Then, each dimension between two given points can be easily measured. As an example. The following figure shows the distance between the two left and right shoulders. (landmarks 11 and 12)

As seen, the measured value is 288.8 millimeters while the real measured distance is 300 by means of the standard metric system.

Figure 8. measuring shoulder width

3. Results

As mentioned, the optical camera used in this study can capture motion data, two-dimensionally. For taking three-dimensional motion information of each point, two cameras are required. Figure 9 shows 2D displacement of all fifteen test points at Left-Right (X-axis) and Superior-Inferior (Y-axis) directions as a function of time. The obtained data will be finally saved as log files. For more clarification, Figures 10 and 11 illustrate the 1D displacement of all fifteen

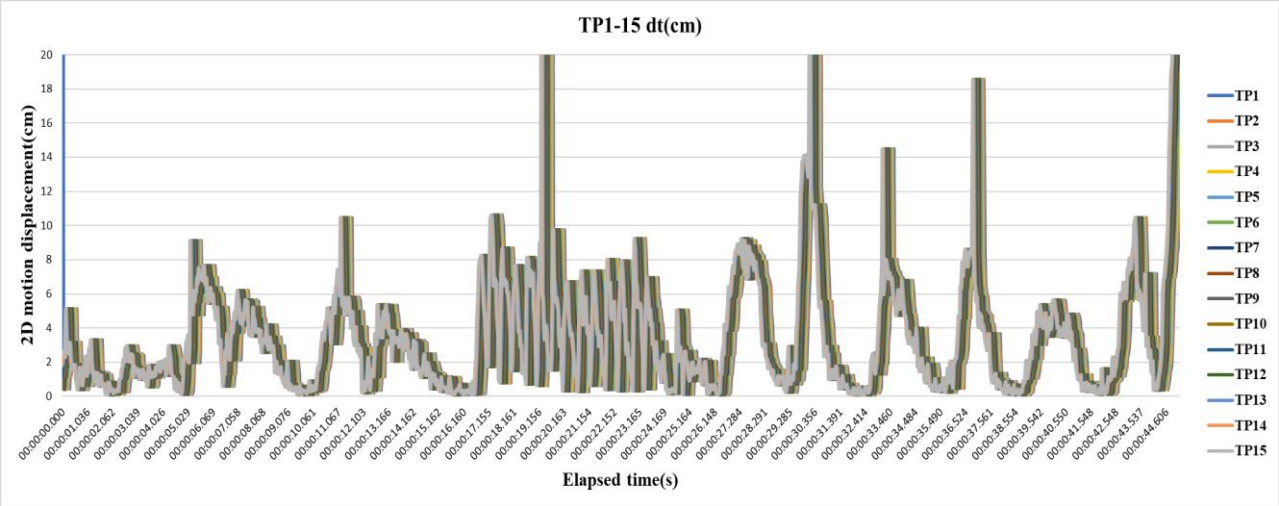

Figure 9. 2D motion displacement of all test points from No. 1 to No. 15

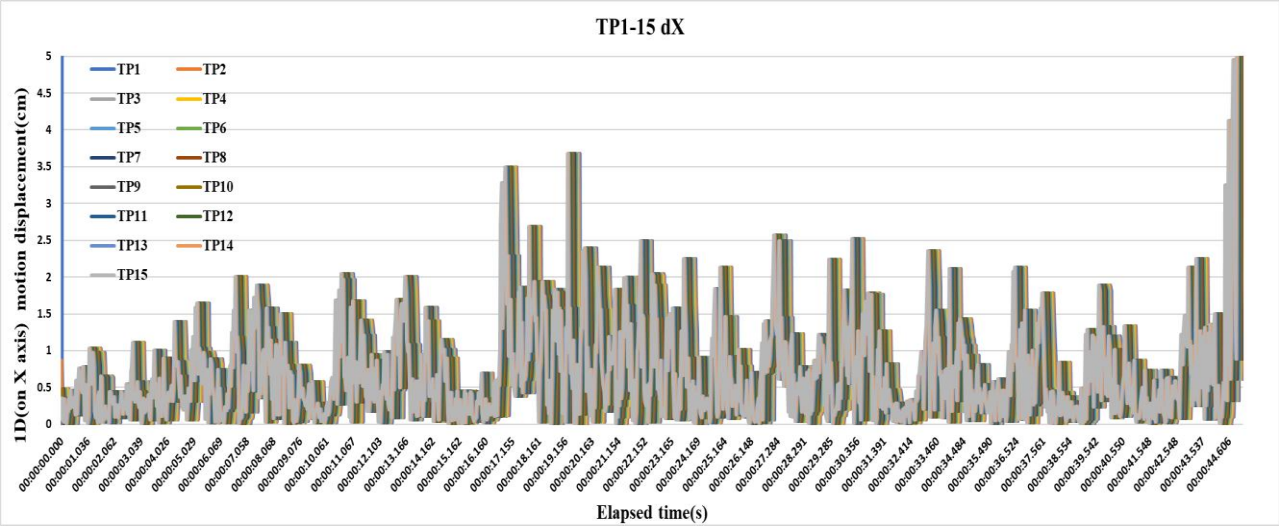

Figure 10. 1D (on X axis) motion displacement of all test points from No. 1 to No. 15

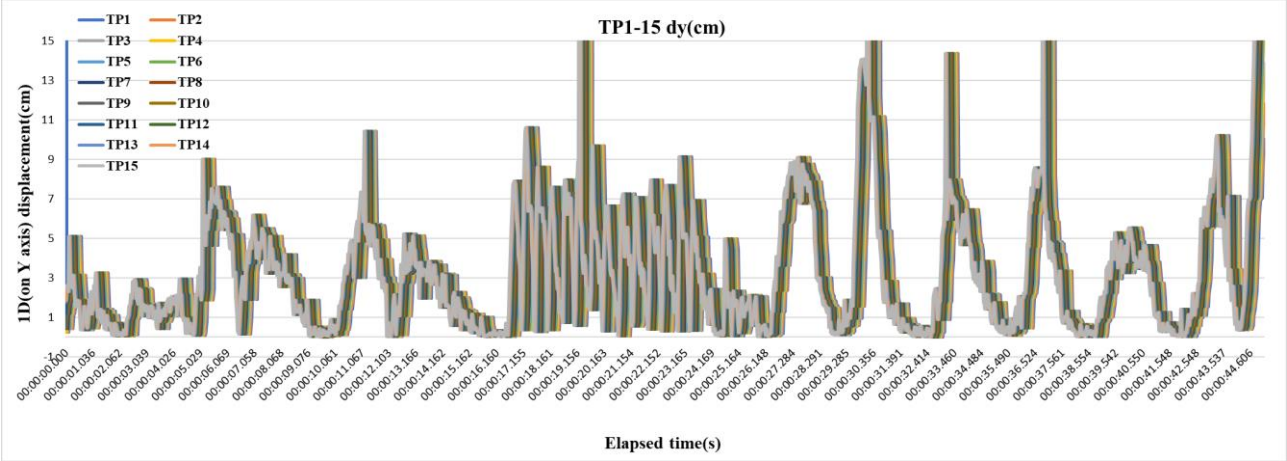

Figure 11. 1D (on Y axis)) motion displacement of all test points from No. 1 to No. 15

points on X and Y axes, separately. As seen in these figures, the amplitude of displacements of the points on the Y-axis is significant regarding to the same displacement on the X-axis. In other words, while

breathing, motion amplitude is almost in the Superior-Inferior direction, which is mainly due to lung region structure and Diaphragm motion direction.

For better visualization, the motion displacement data of test point No. 3 has been chosen versus a specific time period of one minute (Figure 12). As seen in this figure, a typical inhalation and exhalation has been shown (by red color) at two signals. Also, part of the signal marked by green color represents rapid breathing in which the respiratory frequency would be increased, which is obviously noticeable on the graph. The amplitude of this signal depends on the breathing type, which will be normal or deep with various frequencies.

4. Discussion

The main aim of this study is to monitor the chest motion of patients as real time by using a simple strategy applicable at radiotherapy using an external surrogates strategy. An optical cellphone camera that is very common available tool, has been used as hardware system to capture motion information with proper sample rate to track breathing motion as function of time. The captured data were moved to the computer system by means of WiFi. Moreover, a motion tracking algorithm based on optical flow has been developed at Phayton software package. Furthermore, the robust Artificial Intelligence subroutine of Python has been employed for chest region and test point detection. It should be noted that the test points defined in this study are virtual and there is no need for physical external markers for locating on patient's body skin, such as infra-red markers and so on. The proposed method is contactless, that is another novelty of the performed work. Taking into account virtual markers, the minimum cooperation is needed with patients who can be helpful for medical physicians. Using a cellphone camera as a commonly available optical camera for motion tracking of the chest is another robust point of the proposed method due to the availability and costs of such cameras. Since final displacement data are in pixel system, an Aruco marker located on the patient's vest has been used to convert pixels into the standard metric system, such as millimeters. It should be noted that the vest should be tight enough to capture real chest motion with no fault.

The final obtained results represent the motion displacements as 2D and 1D in the left-right and superior-inferior directions of the patient's body. To do this, a volunteer has cooperated with us asking different types of breathing with various amplitudes and frequencies. According to Figures 9 and 10, the end parts of these graphs indicate deep breathing, while the rest of the graphs show normal breathing. By comparing the results, the main displacement with remarkable motion amplitude is almost at superior-inferior direction that is mainly due to the diaphragm organ and the lung anatomical structure. Future studies can be done taking internal tumor motion information by means of X-ray imaging systems and developing an appropriate correlation between chest motion data extracted by our proposed strategy and internal tumor motion using prediction models. Moreover, in order to

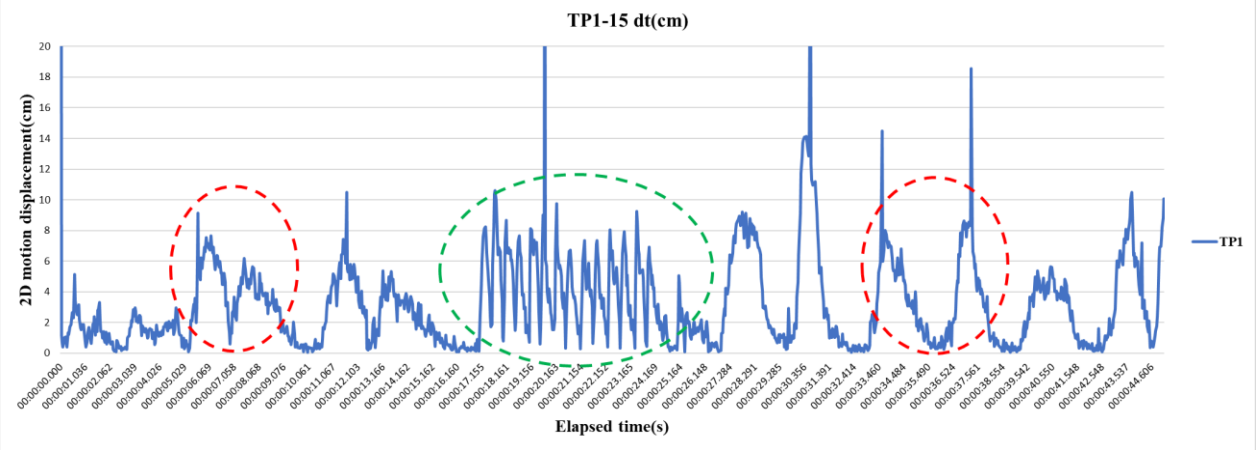

Figure 12. motion displacement of test point No. 3 as a function of time(from left to right: the first red circle represents normal breathing, the green circle in the middle represents rapid breathing at high frequency, and the last red circle shows deep breath, which has the highest amplitude, and there is a pause between two cycles of breathing process)

obtain 3D motion information of the chest area, two optical cameras can be used with different angles.

5. Conclusion

This study includes real-time motion monitoring of the chest area applicable to external surrogates radiotherapy. A commonly available optical camera was used as hardware, and an algorithm was developed in Python to analyze the captured motion data of the chest region. A volunteer was asked to cooperate for testing and validating the proposed strategy. Various types of breathing such as normal and deep breaths, were monitored properly in real time. The proposed method is contactless with proper simplicity and can be suggested to radiotherapy centers for clinical applications.

References

1- Qian Chen *et al.*, "Nanoparticle-Enhanced Radiotherapy to Trigger Robust Cancer Immunotherapy." *Advanced Materials,* https://doi.org/10.1002/adma.201802228 Vol. 31 (No. 10), p. 1802228, 2019/03/01 (2019).

2- Han Ah Lee, Yeon Seok Seo, In-Soo Shin, Won Sup Yoon, Hye Yoon Lee, and Chai Hong Rim, "Efficacy and feasibility of surgery and external radiotherapy for hepatocellular carcinoma with portal invasion: A meta-analysis." *International Journal of Surgery,* Vol. 104p. 106753, 2022/08/01/ (2022).

3- Shervin M. Shirvani *et al.*, "Biology-guided radiotherapy: redefining the role of radiotherapy in metastatic cancer." *The British Journal of Radiology,* Vol. 94 (No. 1117), p. 20200873, 2021/01/01 (2020).

4- Mrcp Frcr M. D. Li Tee Tan Mbbs *et al.*, "Image-guided Adaptive Radiotherapy in Cervical Cancer." *Seminars in Radiation Oncology,* Vol. 29 (No. 3), pp. 284-98, 2019/07/01/ (2019).

5- Adam D. Yock *et al.*, "Robustness Analysis for External Beam Radiation Therapy Treatment Plans: Describing Uncertainty Scenarios and Reporting Their Dosimetric Consequences." *Practical Radiation Oncology,* Vol. 9 (No. 4), pp. 200-07, (2019).

6- Heidi T. Lotz *et al.*, "Tumor motion and deformation during external radiotherapy of bladder cancer." *International Journal of Radiation Oncology*Biology*Physics,* Vol. 64 (No. 5), pp. 1551-58, 2006/04/01/ (2006).

7- Yvette Seppenwoolde *et al.*, "Precise and real-time measurement of 3D tumor motion in lung due to breathing and heartbeat, measured during radiotherapy." *International Journal of Radiation Oncology*Biology*Physics,* Vol. 53 (No. 4), pp. 822-34, 2002/07/15/ (2002).

8- Hendrik Ballhausen, Minglun Li, Ute Ganswindt, and Claus Belka, "Shorter treatment times reduce the impact of intra-fractional motion." *Strahlentherapie und Onkologie,* Vol. 194 (No. 7), pp. 664-74, (2018).

9- ICRU Prescribing, "Recording and reporting photon beam therapy. ICRU Report 50." *Bethesda, MD: International Commission on Radiation Units and Measurements,* (1993).

10- B. De Bari, N. Sellal, and F. Mornex, "[4D-CT scan and radiotherapy for hepatocellular carcinoma: role in the definition of internal target volume (ITV)]." (in fre), *Cancer radiotherapie : journal de la Societe francaise de radiotherapie oncologique,* Vol. 15 (No. 1), pp. 43-48, 2011/02// (2011).

11- Hong Ge, Jing Cai, Chris R. Kelsey, and Fang-Fang Yin, "Quantification and Minimization of Uncertainties of Internal Target Volume for Stereotactic Body Radiation Therapy of Lung Cancer." *International Journal of Radiation Oncology*Biology*Physics,* Vol. 85 (No. 2), pp. 438-43, 2013/02/01/ (2013).

12- Jian-Yue Jin, Munther Ajlouni, Qing Chen, Fang-Fang Yin, and Benjamin Movsas, "A technique of using gated-CT images to determine internal target volume (ITV) for fractionated stereotactic lung radiotherapy." *Radiotherapy and Oncology,* Vol. 78 (No. 2), pp. 177-84, 2006/02/01/ (2006).

13- H. Helen Liu *et al.*, "Assessing Respiration-Induced Tumor Motion and Internal Target Volume Using Four-Dimensional Computed Tomography for Radiotherapy of Lung Cancer." *International Journal of Radiation Oncology*Biology*Physics,* Vol. 68 (No. 2), pp. 531-40, 2007/06/01/ (2007).

14- H. Helen Liu *et al.*, "Evaluation of internal lung motion for respiratory-gated radiotherapy using MRI: Part II—margin reduction of internal target volume." *International Journal of Radiation Oncology*Biology*Physics,* Vol. 60 (No. 5), pp. 1473-83, 2004/12/01/ (2004).

15- F. De Rose *et al.*, "Organs at risk in lung SBRT." *Physica Medica,* Vol. 44pp. 131-38, 2017/12/01/ (2017).

16- Shuichi Nishimura *et al.*, "Toxicities of Organs at Risk in the Mediastinal and Hilar Regions Following Stereotactic Body Radiotherapy for Centrally Located Lung Tumors." *Journal of Thoracic Oncology,* Vol. 9 (No. 9), pp. 1370-76, 2014/09/01/ (2014).

17- Rikiya Onimaru *et al.*, "Tolerance of organs at risk in small-volume, hypofractionated, image-guided radiotherapy for primary and metastatic lung cancers." *International Journal of Radiation Oncology*Biology*Physics,* Vol. 56 (No. 1), pp. 126-35, 2003/05/01/ (2003).

18- Yatman Tsang *et al.*, "Assessment of contour variability in target volumes and organs at risk in lung cancer radiotherapy." *Technical Innovations & Patient Support in Radiation Oncology,* Vol. 10pp. 8-12, 2019/06/01/ (2019).

19- Joseph Hanley *et al.*, "Deep inspiration breath-hold technique for lung tumors: the potential value of target immobilization and reduced lung density in dose escalation." *International Journal of Radiation Oncology*Biology*Physics,* Vol. 45 (No. 3), pp. 603-11, 1999/10/01/ (1999).

20- Paul Keall and G Mageras, "Managing respiratory motion in radiation therapy." *American Association of Physicists in Medicine,* (2004).

21- G. S. Mageras and E. Yorke, "Deep inspiration breath hold and respiratory gating strategies for reducing organ motion in radiation treatment." (in eng), *Semin Radiat Oncol,* Vol. 14 (No. 1), pp. 65-75, Jan (2004).

22- Ahmad Esmaili Torshabi and Leila Ghorbanzadeh, "A study on stereoscopic x-ray imaging data set on the accuracy of real-time tumor tracking in external beam radiotherapy." *Technology in Cancer Research & Treatment,* Vol. 16 (No. 2), pp. 167-77, (2017).

23- Leila Ghorbanzadeh and Ahmad Esmaili Torshabi, "An Investigation into the Performance of Adaptive Neuro-Fuzzy Inference System for Brain Tumor Delineation Using ExpectationMaximization Cluster Method; a Feasibility Study." *Frontiers in Biomedical Technologies,* Vol. 3 (No. 1-2), pp. 8-19, (2016).

24- Leila Ghorbanzadeh, Ahmad Esmaili Torshabi, Jamshid Soltani Nabipour, and Moslem Ahmadi Arbatan, "Development of a synthetic adaptive neuro-fuzzy prediction model for tumor motion tracking in external radiotherapy by evaluating various data clustering algorithms." *Technology in Cancer Research & Treatment,* Vol. 15 (No. 2), pp. 334-47, (2016).

25- Payam Samadi Miandoab, Ahmad Esmaili Torshabi, and Saber Nankali, "Investigation of the optimum location of external markers for patient setup accuracy enhancement at external beam radiotherapy." *Journal of Applied Clinical Medical Physics,* Vol. 17 (No. 6), pp. 32-43, (2016).

26- P Samadi Miandoab, A Esmaili Torshabi, and S Nankali, "Extraction of respiratory signal based on image clustering and intensity parameters at radiotherapy with external beam: A comparative study." *Journal of Biomedical Physics & Engineering,* Vol. 6 (No. 4), p. 253, (2016).

27- Saber Nankali, Ahmad Esmaili Torshabi, and Payam Samadi Miandoab, "A feasibility study on ribs as anatomical landmarks for motion tracking of lung and liver tumors at external beam radiotherapy." *Technology in Cancer Research & Treatment,* Vol. 16 (No. 1), pp. 99-111, (2017).

28- Saber Nankali, Ahmad Esmaili Torshabi, Payam Samadi-Miandoab, and Amin Baghizadeh, "Investigation on performance accuracy of different surrogates in real time tumor tracking at external beam radiotherapy." *Frontiers in Biomedical Technologies,* Vol. 2 (No. 2), pp. 73-79, (2015).

29- S Parande, "A Study on Robustness of Various Deformable Image Registration Algorithms on Image Reconstruction Using 4DCT Thoracic Images." *Journal of Biomedical Physics & Engineering,* Vol. 9 (No. 5), p. 559, (2019).

30- Payam Samadi Miandoab, Ahmad Esmaili Torshabi, Saber Nankali, and Mohammad Reza Rezaie, "A simulation study on patient setup errors in external beam radiotherapy using an anthropomorphic 4D phantom." *Iranian Journal of medical physics,* Vol. 13 (No. 4), pp. 276-88, (2016).

31- Payam Samadi Miandoab, Ahmad Esmaili Torshabi, and Sohelia Parandeh, "Calculation of inter-and intra-fraction motion errors at external radiotherapy using a markerless strategy based on image registration combined with correlation model." *Iranian Journal of medical physics,* Vol. 16 (No. 3), pp. 224-31, (2019).

32- Payam Samadi-Miyandoab, AhmadEsmaili Torshabi, and Saber Nankali, "2D and 3D Optical Flow Based Interpolation of the 4DCT ImageSequences in the External Beam Radiotherapy." *Frontiers in Biomedical Technologies,* Vol. 2 (No. 2), pp. 93-102, (2015).

33- Payam Samadi-Miyandoab, Ahmad Esmaili Torshabi, Saber Nankali, and Mohamadreza Rezai, "The robustness of various intelligent models in patient positioning at external beam radiotherapy." *Frontiers in Biomedical Technologies,* Vol. 2 (No. 1), pp. 45-54, (2015).

34- A. E. Torshabi, Andrea Pella, Marco Riboldi, and Guido Baroni, "Targeting Accuracy in Real-time Tumor Tracking via External Surrogates: A Comparative Study." *Technology in Cancer Research & Treatment,* Vol. 9 (No. 6), pp. 551-61, 2010/12/01 (2010).

35- Ahmad Esmaili Torshabi, Marco Riboldi, Abbas Ali Imani Fooladi, Seyed Mehdi Modarres Mosalla, and Guido Baroni, "An adaptive fuzzy prediction model for real time tumor tracking in radiotherapy via external surrogates." *Journal of Applied Clinical Medical Physics,* Vol. 14 (No. 1), pp. 102-14, (2013).

36- W. R. Brody *et al.*, "Dual-energy projection radiography: initial clinical experience." (in eng), *AJR Am J Roentgenol,* Vol. 137 (No. 2), pp. 201-5, Aug (1981).

37- Rakesh Patel *et al.*, "Markerless motion tracking of lung tumors using dual-energy fluoroscopy." *Medical Physics,* https://doi.org/10.1118/1.4903892 Vol. 42 (No. 1), pp. 254-62, 2015/01/01 (2015).

38- W. E. R. Berkhout, "[The ALARA-principle. Backgrounds and enforcement in dental practices]." (in dut), *Nederlands tijdschrift voor tandheelkunde,* Vol. 122 (No. 5), pp. 263-70, 2015/05// (2015).

39- Stephen V. Musolino, Joseph DeFranco, and Richard Schlueck, "THE ALARA PRINCIPLE IN THE CONTEXT OF A RADIOLOGICAL OR NUCLEAR EMERGENCY." *Health Physics,* Vol. 94 (No. 2), (2008).

40- A. W. K. Yeung, "The 'As Low As Reasonably Achievable' (ALARA) principle: a brief historical overview and a bibliometric analysis of the most cited publications." *Radioprotection,* Vol. 54 (No. 2), p. 103, 2019 (2019).

41- Jessica C. Hsu *et al.*, "Nanoparticle contrast agents for X-ray imaging applications." *WIREs Nanomedicine and Nanobiotechnology,* https://doi.org/10.1002/wnan.1642 Vol. 12 (No. 6), p. e1642, 2020/11/01 (2020).

42- Justine Wallyn, Nicolas Anton, Salman Akram, and Thierry F. Vandamme, "Biomedical Imaging: Principles, Technologies, Clinical Aspects, Contrast Agents, Limitations and Future Trends in Nanomedicines." *Pharmaceutical Research,* Vol. 36 (No. 6), p. 78, 2019/04/03 (2019).

43- Ahmad Zaky Harun, Raizulnasuha Ab Rashid, Khairunisak Ab Razak, Moshi Geso, and Wan Nordiana Wan Abd. Rahman, "Evaluation of Contrast-Noise Ratio (CNR) in contrast enhanced CT images using different sizes of gold nanoparticles." *Materials Today: Proceedings,* Vol. 16pp. 1757-65, 2019/01/01/ (2019).

44- Price Jackson, Selvakannan Periasamy, Vipul Bansal, and Moshi Geso, "Evaluation of the effects of gold nanoparticle shape and size on contrast enhancement in radiological imaging." *Australasian Physical & Engineering Sciences in Medicine,* Vol. 34 (No. 2), pp. 243-49, 2011/06/01 (2011).

45- M. Lafrenière, N. Mahadeo, J. Lewis, J. Rottmann, and C. L. Williams, "Continuous generation of volumetric images during stereotactic body radiation therapy using periodic kV imaging and an external respiratory surrogate." *Physica Medica,* Vol. 63pp. 25-34, 2019/07/01/ (2019).

46- Yao Li, Wumiao Tang, Jiangbing Zhang, Ruirui Bu, Wenchien Hsi, and Yongqiang Li, "Utilization of Diaphragm Motion to Predict the Displacement of Liver Tumors for Patients Treated with Carbon ion Radiotherapy." *Technology in Cancer Research & Treatment,* Vol. 22p. 15330338231164195, 2023/01/01 (2023).

47- Charlotte Remy and Hugo Bouchard, "Adaptive confidence regions for indirect tracking of moving tumors in radiotherapy." *Medical Physics,* https://doi.org/10.1002/mp.15691 Vol. 49 (No. 7), pp. 4273-83, 2022/07/01 (2022).

48- Guangyu Wang *et al.*, "Correlation of optical surface respiratory motion signal and internal lung and liver tumor motion: a retrospective single-center observational study." *Technology in Cancer Research & Treatment,* Vol. 21p. 15330338221112280, (2022).

49- Wang Shuangbao, J. X. Chen, Dong Zegang, and R. S. Ledley, "SMIS - a real-time stereoscopic medical imaging system." in *Proceedings. 17th IEEE Symposium on Computer-Based Medical Systems*, (2004), pp. 197-202.

50- Philip J. Withers *et al.*, "X-ray computed tomography." *Nature Reviews Methods Primers,* Vol. 1 (No. 1), p. 18, 2021/02/25 (2021).

51- Erik Vanegas, Raul Igual, and Inmaculada Plaza, "Piezoresistive Breathing Sensing System with 3D Printed Wearable Casing." *Journal of Sensors,* Vol. 2019p. 2431731, 2019/12/04 (2019).

52- J. Grlica, T. Martinović, and H. Džapo, "Capacitive sensor for respiration monitoring." in *2015 IEEE Sensors Applications Symposium (SAS)*, (2015), pp. 1-6.

53- Tin T. Dang, Khai Q. Nguyen Tran, Hoang M. Le, Khoa Tran, and Anh Dinh, "A Tool Using Ultrasonic Sensor for Measuring Breathing Rate." in *6th International Conference on the Development of Biomedical Engineering in Vietnam (BME6)*, Singapore, (2018): *Springer Singapore*, pp. 139-43.

54- Shekh MM Islam, Olga Boric-Lubecke, and Victor M Lubekce, "Concurrent respiration monitoring of multiple subjects by phase-comparison monopulse radar using independent component analysis (ICA) with JADE algorithm and direction of arrival (DOA)." *IEEE Access,* Vol. 8pp. 73558-69, (2020).

55- Anthony P Addison, Paul S Addison, Philip Smit, Dominique Jacquel, and Ulf R Borg, "Noncontact respiratory monitoring using depth sensing cameras: A review of current literature." *Sensors,* Vol. 21 (No. 4), p. 1135, (2021).

56- M. H. Li, A. Yadollahi, and B. Taati, "Noncontact Vision-Based Cardiopulmonary Monitoring in Different Sleeping Positions." *IEEE Journal of Biomedical and Health Informatics,* Vol. 21 (No. 5), pp. 1367-75, (2017).

57- Carlo Massaroni, Daniel Simões Lopes, Daniela Lo Presti, Emiliano Schena, and Sergio Silvestri, "Contactless Monitoring of Breathing Patterns and Respiratory Rate at the Pit of the Neck: A Single Camera Approach." *Journal of Sensors,* Vol. 2018p. 4567213, 2018/09/23 (2018).

58- M. Mateu-Mateus, F. Guede-Fernández, M. á García-González, J. J. Ramos-Castro, and M. Fernández-Chimeno, "Camera-Based Method for Respiratory Rhythm Extraction From a Lateral Perspective." *IEEE Access,* Vol. 8pp. 154924-39, (2020).

59- Chiara Romano, Emiliano Schena, Sergio Silvestri, and Carlo Massaroni, "Non-Contact Respiratory Monitoring Using an RGB Camera for Real-World Applications." *Sensors*. Vol. 21 (No. 15). DOI: 10.3390/s21155126

60- L. Tarassenko, M. Villarroel, A. Guazzi, J. Jorge, D. A. Clifton, and C. Pugh, "Non-contact video-based vital sign monitoring using ambient light and auto-regressive

models." *Physiological Measurement,* Vol. 35 (No. 5), p. 807, 2014/03/28 (2014).

61- A. Schweikard, H. Shiomi, and J. Adler, "Respiration tracking in radiosurgery without fiducials." *The International Journal of Medical Robotics and Computer Assisted Surgery,* https://doi.org/10.1002/rcs.38 Vol. 1 (No. 2), pp. 19-27, 2005/01/01 (2005).

62- Carlo Massaroni, Andrea Nicolo, Massimo Sacchetti, and Emiliano Schena, "Contactless methods for measuring respiratory rate: A review." *IEEE Sensors Journal,* Vol. 21 (No. 11), pp. 12821-39, (2020).

63- Robert Gilbert, JH Auchincloss Jr, J Brodsky, and W al Boden, "Changes in tidal volume, frequency, and ventilation induced by their measurement." *Journal of Applied Physiology,* Vol. 33 (No. 2), pp. 252-54, (1972).

64- A. Agarwal, S. Gupta, and D. K. Singh, "Review of optical flow technique for moving object detection." in *2016 2nd International Conference on Contemporary Computing and Informatics (IC3I)*, (2016), pp. 409-13.

65- Kiran Kale, Sushant Pawar, and Pravin Dhulekar, "Moving object tracking using optical flow and motion vector estimation." in *2015 4th international conference on reliability, infocom technologies and optimization (ICRITO)(trends and future directions)*, (2015): *IEEE*, pp. 1-6.

66- Jens Klappstein, Tobi Vaudrey, Clemens Rabe, Andreas Wedel, and Reinhard Klette, "Moving object segmentation using optical flow and depth information." in *Pacific-Rim Symposium on Image and Video Technology*, (2009): *Springer*, pp. 611-23.

67- R Revathi and M Hemalatha, "Certain Approach of Object Tracking using Optical Flow Techniques." *International Journal of Computer Applications,* Vol. 53 (No. 8), (2012).